Inorg. Chem. **2002**, *41*, 6614−6622

A Density Functional Study of S_N2 Substitution at Square-Planar Platinum(II) Complexes

Jason Cooper[†] and Tom Ziegler*

Department of Chemistry, University of Calgary, Calgary, Alberta, Canada T2N 1N4

Received April 25, 2002

The energetics and reaction path in a series of S_N2 substitution reactions at square-planar Pt(II) complexes have been studied by the application of density functional theory (DFT). Calculated free energies show excellent correlation with their experimental counterparts, while the enthalpic and entropic contributions individually indicate the presence of weak intermolecular interactions not accounted for in the present model. The nature of the leaving ligand has been shown to be much more significant in determining the activation barrier than that of the entering ligand; it is inferred (and confirmed by analysis of individual bond energies) that the reaction is driven by the dissociation of the leaving ligand, with the entering ligand playing a more passive role. Analysis of the intrinsic reaction coordinate indicates, further, that the trans ligand plays an unexpectedly dynamic role in stabilizing the transition state due to competition between stabilization and the steric effects of the entering and leaving ligands. The cis ligands, by contrast, are shown to move only slightly through the course of the reaction.

Introduction

The mechanism and kinetics of ligand substitution involving square-planar d^8 metal complexes have been studied extensively.[1] Although such reactions have been reported for metals including not only platinum, palladium, and nickel but also rhodium, irridium, and gold, substitutions at platinum centers have enjoyed particular attention due to their exceptionally low rate of reaction. For such systems, experimental reaction enthalpies and entropies, and in some cases the corresponding activation parameters, are available for a wide variety of ligand combinations.[2−4] With respect to comparitive studies involving monodentate ligands, however, the most complete set of experimental data available is that for the hydrolysis, ammoniolysis, and anation reactions of species of the form $Pt(H_2O)_x(NH_3)_yX_{4-x-y}$, where X is either Cl or Br.[5,6]

The available experimental data support a rate law of the form given in eq 1 for substitutions at a square-planar Pt(II) complex, where [N] represents the concentration of the nucleophile and [M] that of the metal complex:

$$\text{rate} = (k_1 + k_2[\text{N}])[\text{M}] \qquad (1)$$

The rate constant k_2 corresponds to a direct S_N2 substitution by the nuclophile (Scheme 1), while k_1 corresponds to the solvent-assisted mechanism, in which a solvent molecule displaces the leaving group and is subsequently displaced by the nucleophile. The effect of the cis and trans ligands on the reaction rate, as well as that of the nucleophile and leaving group, has been extensively reviewed.[1,7] Experimental studies indicate, further, that the majority of these reactions occur by an associative mechanism involving first a weak square-pyramidal encounter complex and, subsequently, a distorted trigonal-bipyramidal transition state, as illustrated in Scheme 2.[8] Here "M" is the metal center, "N" is the nucleophile, "L" is the leaving group, "T" is the trans ligand, and "X" and "Y" are the cis (or "axial") ligands. Theoretical studies indicate that the N−M−L angle in the transition state is relatively small (about 70−85°),[9] with equatorial bonds lengthened and axial bonds very slightly shortened relative to their equilibrium bond lengths.[10]

* To whom correspondence should be addressed. E-mail: ziegler@ucalgary.ca. Fax: (403) 289-9488.
[†] E-mail: jcooper@ucalgary.ca.

(1) Tobe, M. L.; Burgess, J. *Inorganic Reaction Mechanisms*; Longman: Essex, U.K., 1999.
(2) *Inorg. React. Mech. (London)* **1971**, *1*, 145−152.
(3) *Inorg. React. Mech. (London)* **1974**, *3*, 145−155.
(4) *Inorg. React. Mech. (London)* **1977**, *5*, 143−150.
(5) Coe, J. S. *MTP Int. Rev. Sci.: Inorg. Chem., Ser. 2* **1974**, 45−62.
(6) Elding, L. I. *Inorg. Chim. Acta* **1973**, *7*, 581.
(7) Cattalini, L. *Prog. Inorg. Chem.* **1970**, *13*, 263.
(8) Cross, R. J. *Chem. Soc. Rev.* **1985**, *14*, 197−223.
(9) Lin, Z.; Hall, M. B *Inorg. Chem.* **1991**, *30*, 646−651.
(10) Deeth, R. J.; Elding, L. I. *Inorg. Chem.* **1996**, *35*, 5019−5026.

10.1021/ic020294k CCC: $22.00
Published on Web 11/16/2002

Scheme 1. Principal Substitution Mechanisms

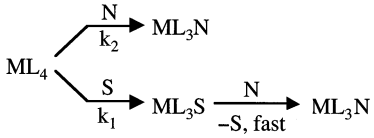

Scheme 2. S_N2 Substitution at a Square-Planar Metal Complex

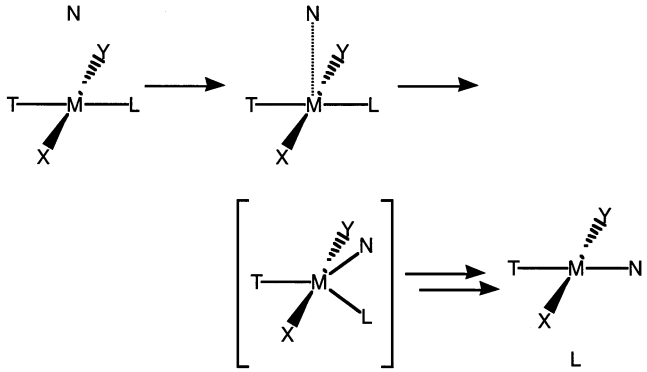

Despite the importance of this class of reactions, and a long history of many experimental and a few theoretical studies, however, the intimate details of the mechanism for S_N2 substitution at a square-planar Pt(II) complex remains a matter of some debate.[8] The general reaction is, for instance, variously reported as involving either a single transition state (Figure 1a) or two transition states separated by an intermediate (Figure 1b).[11]

This study comprises a computational investigation of the reaction path and energetics of the hydrolysis, ammoniolysis, and anation reactions noted above, with X = Cl. It will be assumed only that the initial attack of the nucleophile occurs at the metal center, with no further constraints placed upon the geometry of the transition state. Trends in both reaction path and energetics will be discussed in terms of the nature of the nucleophile and the associated ligands.

Computational Details

Results were obtained from DFT calculations based on the Becke−Perdew exchange-correlation functional,[12−14] using the Amsterdam Density Functional (ADF) program.[15] The standard double-ζ STO bases with one set of polarization functions were applied for H, N, and O atoms, while the standard triple-ζ basis sets were employed for Cl and Pt atoms. The 1s electrons of N and O, as well as the 1s−2p electrons of Cl and the 1s−4f electrons of Pt, were treated as a frozen core. The standard set of auxiliary s, p, d, f, and g STO functions, centered on each nucleus, was used to fit the electron density and the Coulomb and exchange potentials in each SCF cycle. Reported energies include first-order scalar relativistic corrections.[16] Gas-phase electronic enthalpies were calculated from the Kohn−Sham energies. The intrinsic reaction coordinate (IRC) calculated was based on the theory of Fukui.[17] It

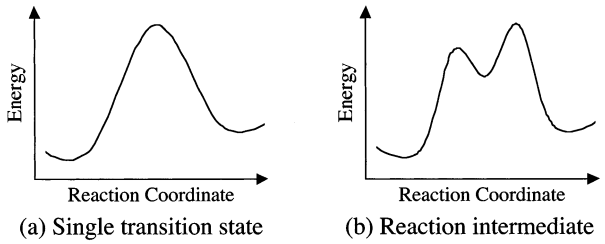

Figure 1. Proposed energy profiles for S_N2 substitution.

was calculated as the union of the paths of steepest descent on the electronic enthalpy surface, in mass-weighted Cartesian coordinates, going from the transition state to the reactants and products. In all values reported, electronic entropy was neglected; standard expressions[18] were used to calculate the remaining gas-phase enthalpic and entropic contributions at nonzero temperature, including the zero-point vibrational contribution.

Thermodynamic parameters for the solvation of the chloride ion were obtained from a recent compilation of experimental values.[19] The remaining solvation enthalpies (included for both single-point calculations and geometry optimizations) were obtained using the COSMO method[20] as implemented in ADF.[21] The solvent excluding surface was used along with an epsilon value of 78.4 for the dielectric constant of water as the solvent. Atomic radii used were 1.39, 1.8, 1.16, 1.4, and 1.3 Å for Pt, Cl, H, N, and O, respectively. Although the Born energy reported by the COSMO model is, strictly speaking, a free energy, the entropic contribution accounts for perhaps 2% of the total energy.[22] The solvation enthalpy was therefore taken as the difference between the gas-phase energy and that calculated using the COSMO solvation model.

For the purposes of calculating the remaining solvation entropies, the solvation process was broken into three steps, following Wertz.[23] Here, the solute in its gas phase is first compressed to the molar volume of the solvent. The compressed solute gas then loses the same fraction of its entropy as would be lost by the solvent in going from gas (at its liquid-phase density) to liquid. Finally, the solute gas is expanded to the density of the desired solution (i.e., 1.0 L/mol).

The entropy change for the first and third steps, which are strictly changes in molar volume, is given by $\Delta S = R \ln V_{m,f}/V_{m,i}$, where $V_{m,f}$ is the final molar volume and $V_{m,i}$ is its initial value. The entropy fraction α lost in the second step can be determined from the absolute entropies of the solvent in its gas ($S_{gas}°$) and liquid ($S_{liq}°$) phases, as shown in eq 2, taking care to include again the change in molar volume.

Substituting the appropriate parameters for water,[24] we have $\alpha = -0.46$. The sum of the entropy changes accompanying each of the three steps then gives the total solvation entropy; at a temperature of 298.15 K, we have (again, for water) eq 3.

It is convenient that (by chance) the constant terms in eq 3 very nearly cancel on expansion, and the solvation entropy in water can therefore be approximated in more qualitative discussions as 50% of the gas-phase entropy, with the opposite sign.

(11) Burdett, J. K. *Inorg. Chem.* **1977**, *16*, 3013−3025.
(12) Becke, A. *Phys. Rev. A* 1988, *38*, 3098.
(13) Perdew, J. P. *Phys. Rev. B* **1986**, *34*, 7406.
(14) Perdew, J. P. *Phys. Rev. B* **1986**, *33*, 8822.
(15) Te Velde, G.; Bickelhaupt, F. M.; Baerends, E. J.; van Gisbergen, S.; Guerra, C. F.; Snijders, J. G.; Ziegler, T. *J. Comput. Chem.* **2001**, *22*, 931.
(16) Ziegler, T.; Tschinke, V.; Baerends, E. J.; Snijders, J. G.; Ravenek, W. *J. Phys. Chem.* **1989**, *93*, 3050.
(17) Fukui, K. *Acc. Chem. Res.* **1981**, *14*, 363.
(18) McQuarrie, D. A. *Statistical Thermodynamics*; Harper: New York, 1973.
(19) Fawcett, W. R. *J. Phys. Chem. B* **1999**, *103*, 11181.
(20) Klamt, A.; Schuurmann, G. *J. Chem. Soc., Perkin. Trans.* **1993**, *2*, 799.
(21) Pye, C. C.; Ziegler, T. *Theor. Chem. Acc.* **1999**, *101*, 396.
(22) Dasent, W. E. *Inorganic Energetics*; Penguin: Middlesex, U.K., 1970.
(23) Wertz, D. H. *J. Am. Chem. Soc.* **1980**, *102*, 5316.
(24) Lide, D. R., Ed. *CRC Handbook of Chemistry and Physics*, 76th ed.; CRC Press: New York, 1995.

$$\alpha = \frac{S_{liq}^{\circ} - (S_{gas}^{\circ} + R \ln V_{m,liq}/V_{m,gas})}{(S_{gas}^{\circ} + R \ln V_{m,liq}/V_{m,gas})} \quad (2)$$

$$\Delta S_{sol} = (-14.3 \text{ cal·mol}^{-1}\text{·K}^{-1}) - 0.46(S^{\circ} - 14.3 \text{ cal·mol}^{-1}\text{·K}^{-1}) + (7.98 \text{ cal·mol}^{-1}\text{·K}^{-1}) \quad (3)$$

Results and Discussion

The reactions studied here are summarized in Figure 2. They have been studied extensively by experimental techniques, and reliable kinetic data are therefore available. Complexes in Figure 2 are represented in a manner similar to that used by Elding,[25] with H_2O and NH_3 represented by "O" and "N", respectively. Reactions 1−9 are hydrolysis reactions, reactions 10−15 are ammoniolysis reactions analogous to the hydrolysis reactions 1−6, and reactions 1′−15′ are anation reactions.

Classification of Reactions. Calculated thermodynamic parameters, with and without the solvation contribution, and the corresponding experimental values in aqueous solution[5] are summarized in Table 1. The reactions, numbered according to Figure 2, are sorted according to the transition state involved, the numeral identifying the equatorial ligands (Chart 1) and the letter identifying the axial ligands (Chart 2). We will discuss, first, trends in the reaction enthalpies and entropies individually before making a comparison of the calculated reaction free energies to experimental values.

Heat of Reaction in Gas Phase and in Solution. The calculated gas-phase reaction enthalpies in Table 1 are determined almost entirely by the effect of Coulomb interactions between the chloride ion and the product metal complex. Values range from about −50 kcal/mol for reactions giving a singly negative product complex (reaction 1) to about +225 kcal/mol for reactions giving a doubly positive product complex (reaction 6). This trend is also seen in solution, where it determines the trend in ΔH between reactions for which the transition state composition differs only in the nature of the axial ligands. The relative strength of the Pt−E, Pt−L, and Pt−T bonds, however, becomes equally important in the determination of ΔH in solution. Thus, in solution, reactions 1−9, in which Cl is displaced by H_2O, are calculated to be endothermic while reactions 10−15 (displacement of Cl by NH_3) are calculated to be exothermic. NH_3 is therefore predicted to give the strongest metal−ligand bond of the three, followed by Cl, and finally H_2O. The calculated reaction enthalpies indicate that the Pt−NH_3 bond is about 12 kcal/mol stronger than the Pt−Cl bond, while the Pt−H_2O bond is about 8 kcal/mol weaker than the Pt−Cl bond.

Translational, Rotational, and Vibrational Contributions to Entropy of Reaction. For its part, the gas-phase entropic contribution can be divided into translational, rotational, and vibrational components. The metal complexes in Figure 2 are geometrically similar to one another, each containing a platinum center surrounded by a set of four ligands. The heaviest ligand is only twice the mass of the lightest, and the longest metal−ligand bond only 15% longer than the shortest. Translational entropy, which varies as the logarithm of the molecular mass, and rotational entropy, which varies as the sum of the logarithms of the principle moments of inertia, therefore differ little among the product and reactant complexes. Due also to the similarity of the free ligand masses, the change in translational entropy is therefore smaller than 2 cal/(K/mol) in each case. Further, it follows that the change in rotational entropy stems almost entirely from the difference in rotational entropy between the nucleophile (H_2O or NH_3) and the leaving group (chloride, which has zero rotational entropy) and is uniformly equal to about −10 cal/(K/mol) (the approximate rotational entropy of the nucleophiles).

Vibrational entropy is negligible for the nucleophile and leaving group, which are either atomic (Cl^-) or contain very stiff bonds (H_2O or NH_3). Change in vibrational entropy therefore arises primarily from an increase in the number of vibrational degrees of freedom in the complex on replacement of an atomic ligand with a molecular one, with a smaller contribution arising from the difference in bond strength between the two. Trends in the total change in gas-phase entropy follow those for the latter contribution, which varies most strongly between reactions, while the absolute values are dominated by the much stronger rotational contribution and are therefore all about −10 cal/(K/mol).

Solvation Contribution to Entropy of Reaction. In solution, the entropy of reaction is found to be about +5 cal/(K/mol) in all cases. This is due to two factors: first, a reduction from the gas-phase value by about 50%; second, a contribution of +10 cal/(K/mol) due to the disruptive effects of the product cloride ion on the local structure of the solvent, calculated as the difference between the solvation entropy as determined by the method of Wertz (−16 cal/(K/mol)) and that observed experimentally (−6 cal/(K/mol)). This phenomenon is especially pronounced in aqueous solutions, such as those considered here, due to the extensive hydrogen bonding in pure water.[19] The entropies of reaction in solution are also found to be more uniform than their gas-phase counterparts due to a reduction of the gas-phase variations by the same factor of 50% employed above.

Free Energy of Reaction. The calculated free energies of reaction correlate very well with the experimental values, with a systematic overestimation by about 1.2 kcal/mol and an rms statistical error of about 1.3 kcal/mol. It is therefore surprising that the calculated enthalpies and entropies of reaction differ quite significantly from their experimental values. Reactions 3 and 8 serve as a particularly clear example. Differing only in the replacement of a cis H_2O ligand with an NH_3, the two reactions give experimental free energies which are both similar to one another and also in good agreement with the calculated values. The experimental reaction enthalpy for reaction 3, however, is 6 kcal/mol higher than that for reaction 8, while the corresponding difference in entropies is 17 cal/(K/mol), in contrast to the calculated values, which differ only slightly between the two reactions. It seems unlikely that the experimental values are in error (kinetic data for reaction 8, for instance,[25] were taken

(25) Elding, L. I. *Acta Chem. Scand.* **1970**, *24*, 1527.

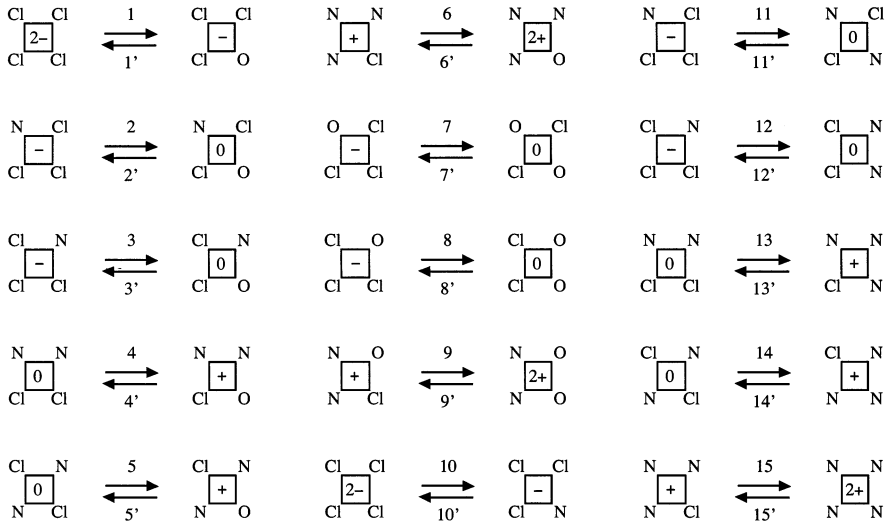

Figure 2. Model reactions.

Table 1. Experimental and Calculated Enthalpies, Entropies, and Free Energies of reaction

		gas phase[c]			with solvation[c]			expt[c,d]		
reacn[a]	TS[b]	ΔS	ΔH	ΔG	ΔS	ΔH	ΔG	ΔS	ΔH	ΔG
1	1a	−7.61	−44.34	−42.07	6.09	3.18	1.37	2	3	2.0
8	1b	−7.58	41.79	44.05	6.11	7.11	5.29	−7	2	4.4
3	1c	−9.69	41.79	44.68	4.96	6.63	5.15	10	8	5.0
5	1f	−10.80	140.83	144.05	4.35	12.19	10.89	−5	3	4.3
10	2a	−8.91	−60.55	−57.90	5.39	−16.55	−18.15			
12	2c	−9.86	31.62	34.56	4.87	−12.27	−13.72			
14	2f	−12.44	121.08	124.79	3.46	−10.73	−11.76			
2	3a	−10.32	35.42	38.49	4.62	5.66	4.28	−6	0	1.8
4	3c	−2.68	124.49	125.29	8.78	7.32	4.70	−2	3	3.6
9	3e	−15.44	226.66	231.27	1.82	7.55	7.01			
6	3f	−5.65	222.99	224.67	7.16	10.46	8.32	−23	−2	4.9
11	4a	−7.46	15.85	18.07	6.18	−13.96	−15.81			
13	4c	−10.04	105.31	108.30	4.77	−12.42	−13.85			
15	4f	−4.38	199.06	200.36	7.86	−8.16	−10.50			
7	5a	−10.21	44.45	47.50	4.68	6.84	5.44	−10	1	4.2

[a] Reaction numbers according to Figure 2. [b] Numeral indicates ligand combination in the equatorial plane (Chart 1); letter indicates ligand combination in the axial positions (Chart 2). [c] ΔS in cal/(K/mol); ΔH in kcal/mol; ΔG in kcal/mol (at 298.15 K). [d] Reference 5.

Chart 1. Possible Ligand Combinations in the Equatorial Plane of the Transition State

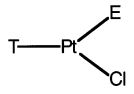

1. T=Cl, E=H_2O
2. T=Cl, E=NH_3
3. T=NH_3, E=H_2O
4. T=NH_3, E=NH_3
5. T=H_2O, E=H_2O

Chart 2. Possible Ligand Combinations in the Axial Positions of the Transition State

a. (Cl, Cl)
b. (Cl, H_2O)
c. (Cl, NH_3)
d. (H_2O, H_2O)
e. (H_2O, NH_3)
f. (NH_3, NH_3)

between 15 and 35 °C, spanning a factor-of-10 range in the forward and reverse reaction rates and giving very linear Arrhenius plots); a reexamination of the model is in order at this point.

Enthalpy−Entropy Compensation. The phenomenon of enthalpy−entropy compensation has been studied extensively.[26] Of possible importance in the present case is compensation between the enthalpic and entropic contributions in weak intermolecular interactions.[27] We have neglected, in the present model, a number of such interactions including weak association of the chloride ion with the product complex. In all but two of the reactions studied, the product complex is either neutral or positively charged; such interactions might therefore be expected to be significant and would act to lower both the reaction enthalpy and entropy, while leaving the free energy unchanged. Enthalpy−entropy compensation therefore might account for the almost systematic overestimation of both parameters in this study.

Furthermore, it has been shown that the explicit solvent−solvent interaction terms of the solvation entropy and enthalpy contributions (which are neglected in a continuum model of solvation) cancel in the expression for the free energy of solvation.[28] It is reasonable to expect that such interactions might play a role in the experimental differences noted between reactions 8 and 3. In the former case, the product complex contains cis aqua ligands and might be expected to serve as a template for hydrogen bonding within the solvent. This is not true in the latter case. Accordingly,

(26) Liu, L.; Guo, Q.-X. *Chem. Rev.* **2001**, *101*, 673.

(27) Williams, D. H.; Westwell, M. S. *Chem. Soc. Rev.* **1998**, *27*, 57.
(28) Yu, H.-A.; Karplus, M. *J. Chem. Phys.* **1988**, *89*, 2366.

Table 2. Average Ligand Bond Lengths for Ground-State Species

	bond length (Å)		
trans group	H_2O	Cl	NH_3
H_2O	2.06	2.30	2.02
Cl	2.11	2.34	2.05
NH_3	2.12	2.35	2.06

the enthalpy and entropy of reaction are observed to be much lower for reaction 8 than for reaction 3.

It is important, therefore, not to devalue the calculated enthalpy and entropy values entirely, for although they differ from the corresponding experimental values, trends in the calculated values may nevertheless reflect important differences in the true reaction energetics. The preceding discussion of the calculated enthalpies and entropies may remain relevant, and in what follows, we will continue to discuss these properties individually as well as discussing their cumulative effect.

Parameters Influencing Ground-State Geometry. Pt−L bond lengths for the species in Figure 2 depend most strongly on the identity of the ligand L and of the group trans to it. Table 2 summarizes the average bond lengths for each case; individual cases in each set differ by less than 0.01 Å from the average values. Variation of the trans group shows a strong effect on ligand bond length which is independent of the identity of the ligand. The calculated trans influence—the weakening of a ligand bond due to competition with the group trans to it—follows the expected[1] order NH_3 > Cl > H_2O. Ammonia, which we have shown in the previous section to be the strongest bound ligand of the three, is predicted to compete most effectively as a trans ligand, giving the longest bonds for ligands trans to it. Water, the weakest bound of the three, competes least effectively and gives the shortest bonds for such ligands.

Comparison of Calculated Kinetic Parameters to Experimental Values. Table 3 compares the entropies, enthalpies, and free energies of activation—calculated in the gas phase and in aqueous solution—to experimental values (in aqueous solution) for the forward reactions, while Table 4 compares the corresponding parameters for the reverse reactions. Transition state structures were determined from the energy maximum of a linear transit along the bond length difference coordinate $\Delta R = R(\mathrm{Pt-E}) - R(\mathrm{Pt-Cl})$ (cf. Chart 1). The optimized structures were shown to have exactly one imaginary frequency, as expected for a transition state species. Note that the calculated barriers for the hydrolysis reactions investigated are systematically higher than those for the corresponding ammoniolysis reactions; we can therefore assert that none of the ammoniolysis reactions occur primarily by the solvent-mediated mechanism (e.g. Scheme 3) in aqueous solution.

Influence of Entering and Leaving Ligands on Enthalpy of Activation. Variation of the entering ligand (that is, of "E" for the forward reactions) has only a small effect on the activation enthalpic barrier both experimentally and theoretically. Comparing reactions 1 and 10, for instance (which differ only in the entering ligand involved), we see a difference of only 0.4 kcal/mol in the calculated value of $\Delta H^{\ddagger}$ in solution. By contrast, variation of the leaving ligand ("E" for the reverse reactions) has a profound impact on the calculated activation barrier, though a similar comparison is not possible for the experimental values. Comparing now reactions 1′ and 10′, we see a difference of almost 20 kcal/mol favoring the reaction in which water (the weaker of the two "E" groups) is the leaving ligand. These trends are repeated for all reaction pairs in which a group 1 transition state (Chart 1) is replaced by the corresponding group 2 transition state, or a group 3 transition state by a group 4 transition state. The average difference in the calculated enthalpic barriers between those reactions with H_2O as an entering ligand and those with NH_3 in the same position is 2.3 kcal/mol (4.2 kcal/mol experimentally) and always favors NH_3. The corresponding calculated difference with H_2O and NH_3 as leaving ligands gives an average value of 18 kcal/mol and always favors H_2O.

That variation in the leaving ligand has the greater effect on enthalpic barrier indicates that its dissociation from the complex plays a more important role in the intimate mechanism than does the approach of the entering ligand. It is therefore likely that the entering ligand plays a more passive role and (1) is axially bound to the complex before the leaving ligand begins to dissociate or (2) moves in from the first solvation shell as the leaving ligand begins to dissociate.[29] Although our IRC studies (discussed later) do indicate that the entering ligand approaches from an axial position in some cases, we have been unable to optimize a structure in which the entering ligand was even weakly bound there. It seems more likely, therefore, that the latter is true.

Bond Making and Bond Breaking in the Transition State. This picture is supported by a bond-energy analysis on the reactant, product, and transition state for reactions 1 and 10. For the purposes of calculating bond energies, the entering and leaving ligands were removed individually from the product and reactant, respectively, and from the transition state, and the bonding energy was calculated for the resultant complexes without geometry reoptimization. From the sum of this energy and that of the ligand was subtracted the energy of the unaltered complex to give an estimate of the bond energy attributable to each ligand alone. In each case, the bond energy of both entering and leaving groups was calculated to be less than 2 kcal/mol in the transition state, compared to a bond energy in the ground-state species of between 12 and 30 kcal/mol depending on the ligand examined. The energy change on going from reactant to transition state is therefore dominated by the breaking of the Pt−Cl bond (which, in both cases, loses about 90% of its bond energy in this period while the entering ligand achieves only 10% of its final bond energy). Similarly, the energy change on going from transition state to product is dominated by the formation of the Pt−E bond. For both forward and reverse reactions, then, the activation process is dominated by bond breaking, the bond to the entering ligand becoming significant only very near the transition state. Even so, the process is only weakly associative; taking these together, it

(29) Langford, C.; Gray, H. *Ligand Substitution Processes*; Benjamin: New York, 1966.

Table 3. Comparison of Activation Parameters for the Forward Reactions

		gas phase[a]			with solvation[a]			expt[a,b]		
reacn	TS	$\Delta S^{\ddagger}$	$\Delta H^{\ddagger}$	$\Delta G^{\ddagger}$	$\Delta S^{\ddagger}$	$\Delta H^{\ddagger}$	$\Delta G^{\ddagger}$	$\Delta S^{\ddagger}$	$\Delta H^{\ddagger}$	$\Delta G^{\ddagger}$
1	1a	−30.47	7.57	16.65	−16.76	17.44	22.44	−8	21	23.4
8	1b	−29.88	11.31	20.22	−16.44	20.75	25.65	−11	20	23.3
3	1c	−28.24	19.23	27.65	−15.54	20.97	25.60	−9	20	22.7
5	1f	−31.94	20.81	30.34	−17.56	20.23	25.47	−11	19	22.3
10	2a	−26.94	19.91	27.95	−14.84	17.04	21.46	−22	16	22.6
12	2c	−25.06	20.38	27.85	−13.81	17.31	21.43	−18	16	21.4
14	2f	−33.74	20.35	30.41	−18.54	16.37	21.90	−33	10	19.8
2	3a	−27.46	18.91	27.10	−15.12	20.58	25.09	−30	15	23.9
4	3c	−31.09	23.55	32.82	−17.10	21.14	26.23	−14	20	24.2
9	3e	−40.45	30.92	42.98	−22.20	21.10	27.72	−11	20	23.3
6	3f	−33.49	24.49	34.47	−18.40	21.77	27.26	−18	18	23.4
11	4a	−26.34	21.71	29.56	−14.51	19.37	23.69	−18	18	22.9
13	4c	−24.23	18.52	25.75	−13.36	20.02	24.00	−15	18	22.5
1	4f	−20.82	13.65	19.86	−11.50	19.18	22.61	−15	17	21.5
7	5a	−31.30	19.31	28.64	−17.21	24.08	29.21	−12	24	27.6

[a] ΔS in cal/(K/mol); ΔH in kcal/mol; ΔG in kcal/mol (at 298.15 K). [b] Reference 5.

Table 4. Comparison of Activation Parameters for the Reverse Reactions

		gas phase[a]			with solvation [a]			expt[a,b]		
reacn	TS	$\Delta S^{\ddagger}$	$\Delta H^{\ddagger}$	$\Delta G^{\ddagger}$	$\Delta S^{\ddagger}$	$\Delta H^{\ddagger}$	$\Delta G^{\ddagger}$	$\Delta S^{\ddagger}$	$\Delta H^{\ddagger}$	$\Delta G^{\ddagger}$
1′	1a	−22.86	51.90	58.72	−22.85	14.26	21.07	−10	18.4	21.4
8′	1b	−22.30	−30.48	−23.83	−22.54	13.63	20.35	−4	17.7	18.9
3′	1c	−18.55	−22.56	−17.03	−20.50	14.34	20.46	−19	12	17.7
5′	1f	−21.14	−120.01	−113.71	−21.91	8.04	14.58	−6	16.2	18.0
10′	2a	−18.04	80.46	85.84	−20.22	33.59	39.62			
12′	2c	−15.20	−11.23	−6.70	−18.68	29.59	35.15			
14′	2f	−21.30	100.73	−94.38	−22.00	27.10	33.66			
2′	3a	−17.14	−16.50	−11.39	−19.74	14.92	20.81	−24	15	22.2
4′	3c	−28.41	−100.94	−92.47	−25.88	13.82	21.54	−12	17	20.6
9′	3e	−25.00	−195.74	−188.29	−24.02	13.55	20.71			
6′	3f	−27.84	−198.50	−190.20	−25.57	11.31	18.93	5	20	18.5
11′	4a	−18.89	5.86	11.49	−20.69	33.33	39.50			
13′	4c	−14.20	−86.79	−82.56	−18.13	32.44	37.85			
15	4f	−16.44	−185.41	−180.50	−19.35	27.34	33.11			
7′	5a	−21.08	−25.14	−18.86	21.88	17.24	23.77	−2	22.8	23.4

[a] ΔS in cal/(K/mol); ΔH in kcal/mol; ΔG in kcal/mol (at 298.15 K). [b] Reference 5.

Scheme 3. Solvent-Mediated Pathway for Reaction 10

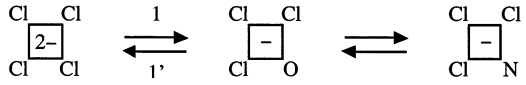

might be equally well described as following a facilitated dissociative mechanism.

Influence of Trans Ligand on Enthalpy of Activation. Variation of the trans ligand is found to have an effect on the enthalpic barrier which is of the same magnitude as that noted for variation of the entering ligand, the so-called trans effect experimentally following the order $NH_3 > Cl > H_2O$, where all other ligands remain unchanged. Similarly, in solution, reactions with Cl as the trans group are calculated to be favored enthalpically by an average of 1.7 kcal/mol over the corresponding reactions with NH_3 as the trans group and by 4.8 kcal/mol over those with H_2O as the trans group. The trans influence, discussed earlier, contributes substantially to this effect by modifying the strength of the bond between the leaving ligand and the metal center. It is therefore important to the trans effect that (as already demonstrated) the reaction kinetics are sensitive to the strength of the bond to the leaving ligand. The relative strength of Cl as a trans ligand despite its moderate trans influence is in excellent agreement with experiment and can be attributed to a second contribution, arising from the delocalization of charge through π-bonding between the trans ligand and the metal.[1] The enthalpic trans effect order is reflected in the calculated free energies and is again in excellent agreement with experiment.

Translational, Rotational, and Vibrational Contributions to Entropy of Activation. By an argument similar to that presented for the corresponding reaction parameters, the translational part of the gas-phase entropy of activation is expected to stem almost entirely from the loss of the translational entropy of the nucleophile (about −35 cal/(K/mol)). Similarly, the change in gas-phase rotational entropy stems almost entirely from the loss of rotational freedom in the nucleophile and is therefore near zero for the reverse (anation) reactions and about −10 cal/(K/mol) for the forward (hydrolysis and amoniolysis) reactions. The degrees of freedom lost are exchanged for vibrations, resulting in an increase in the gas-phase vibrational entropy by about 15 cal/(K/mol). The balance of these effects gives a gas-phase activation entropy of about −30 cal/(K/mol) for the forward reactions and about −20 cal/(K/mol) for the reverse, the difference between the two resulting from loss of the rotational entropy of the nucleophile in the reverse reactions. Variations in each are (as was the case for the reaction entropies) due

Scheme 4. Indirect Mechanism for Reaction 7

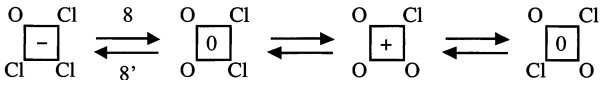

Table 5. Transition State Geometries

		bond angles (deg)		bond lengths (Å)		
TS	charge	T−M−E	T−M−Cl	T−M	E−M	Cl−M
1a	−2	150.8	143.8	2.31	2.61	2.92
1b	−1	149.0	143.2	2.30	2.63	2.88
1c	−1	151.5	142.1	2.32	2.57	2.88
1f	0	151.6	141.4	2.32	2.52	2.84
2a	−2	135.8	148.3	2.36	2.56	2.67
2c	−1	133.2	147.5	2.37	2.52	2.64
2f	0	133.7	147.3	2.38	2.51	2.63
3c	0	150.1	144.4	2.02	2.59	2.89
3e	+1	149.9	143.7	2.03	2.53	2.85
3f	+1	149.9	143.7	2.04	2.52	2.85
4a	−1	138.2	148.3	2.05	2.60	2.72
4c	0	137.2	148.0	2.06	2.59	2.66
4f	+1	128.3	155.3	2.07	2.56	2.63
5a	1	150.6	141.6	2.12	2.48	2.80

to differences in the vibrational contribution and are on the order of ±5 cal/(K/mol).

Solvation Contribution to Entropy of Activation. For the forward reactions, the solvation contribution to the activation entropy is about 50% of the gas-phase value, or +15 cal/(K/mol). In the absence of other factors, one would similarly expect the solvation contribution for the reverse reactions to be about +10 cal/(K/mol). Instead, the disruptive effects of the reactant Cl^- anion, noted previously, very nearly cancel this contribution; the solvation contribution for the reverse reactions is therefore small. The resulting solution-phase activation entropies are about −15 and −20 cal/(K/mol) for the forward and reverse reactions, respectively.

Particularly in solution (where variations in the activation entropy are reduced, as before, by a factor of about 50%), variations in the activation entropies are much smaller in relative magnitude than those in the activation enthalpies. Trends in the free energy of activation therefore principally follow those noted above in its enthalpic part. As was the case for the reaction free energies, the calculated activation free energies agree very well with experimental values where the latter are available. This agreement is especially remarkable in light of the suggestion by Elding[25] that reaction 7, in particular, occurs only negligibly by the direct process shown in Figure 2, instead proceeding predominantly by an indirect mechanism (Scheme 4).

Influence of Entering and Leaving Ligands on Transition State Geometry. We turn, finally, to the calculated structures of the transition states, summarized in Table 5. The first trend here is a series of systematic differences between groups 1, 3, and 5 of Chart 1 (for which E = H_2O) and groups 2 and 4 (for which E = NH_3). In the former case, Pt−Cl bond lengths are larger, T−Pt−Cl angles smaller, and T−Pt−E angles larger than in the latter. More particularly, in the former case the T−Pt−Cl angle is smaller than the T−Pt−E angle, while in the latter case the opposite is true. These observations are illustrated for clarity in Figure 3 and indicate a late transition state where H_2O is the entering ligand and an early transition state where NH_3 is the entering ligand. This difference arises from the relative strengths of the metal−ligand bonds, as determined earlier (NH_3 > Cl > H_2O) and can be rationalized through the Hammond postulate. Figure 4 shows the enthalpic profiles for reactions 1 and 10. For reaction 1, which is endothermic, the product is higher in energy. and therefore closer in energy to the transition state, than the reactant. By the Hammond postulate, we therefore expect the transition state to more closely resemble the product, as is observed. By contrast, for reaction 10 (which is exothermic), the reactant is higher in energy; an early transition state is the result.

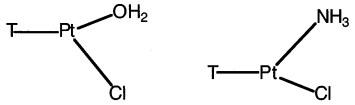

Figure 3. Schematic representation of the transition state geometries. (Only equatorial ligands are shown.)

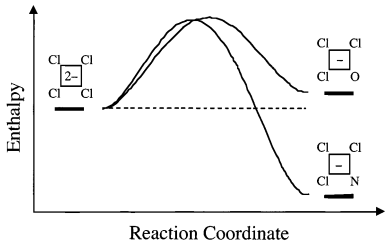

Figure 4. Schematic reaction profiles for reactions 1 and 10.

Influence of Charge on Transition State Geometry. The effect of charge on the transition state geometry can be examined by the comparison of transition states having the same equatorial ligands but different axial ligands. As charge goes from positive to negative values (that is, as H_2O and NH_3 axial ligands are replaced by Cl^-), the Pt−T bond length is generally decreased slightly while the Pt−E and Pt−Cl bond lengths are increased more substantially. The presence of a more negative charge in the reactant weakens the bond to the Cl^- leaving group by Coulomb repulsion. This results in both a longer Pt−Cl bond and an earlier transition state (and therefore a longer Pt−E bond). Steric repulsion between the trans group and these ligands is thereby reduced, and the trans bond is shortened, stabilizing the transition state and completing the observed trends.

Intrinsic Reaction Coordinate. Supplemental to the data in Table 5, the IRC has been calculated for reactions 1 and 10 (the hydrolysis and ammoniolysis of $PtCl_4^{2-}$, respectively). It should be noted, first, that no evidence was found for the existence of a reaction intermediate in either case. The range over which the IRC was studied leaves open the possibility of a weakly bound encounter complex between the entering ligand (or leaving ligand) and the reactant (or product); however, our attempts at obtaining an optimized structure for such a complex indicate that it does not exist. Figure 5 shows the variation of metal−ligand bond lengths along the IRC for reaction 10. The reaction coordinate indicated represents the distance from the transition state in mass-weighted coordinates. The IRC shown exhibits a number of features which are common to both reactions; we will discuss the role of each ligand in turn.

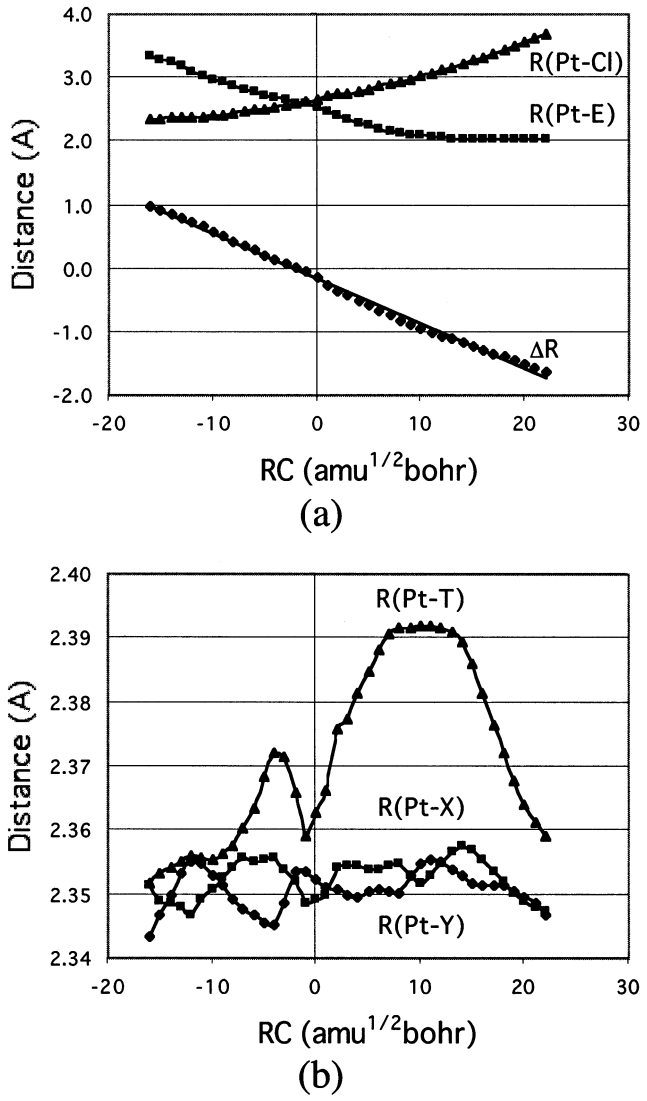

Figure 5. IRC for reaction 10: (a) changes in the Pt−E and Pt−Cl bond lengths and in the bond length difference coordinate (ΔR) as a function of the reaction coordinate; (b) changes in the Pt−T, Pt−X, and Pt−Y bond lengths as a function of the reaction coordinate.

The entering ligand is predicted to approach (and the leaving ligand depart) at an angle of about 90−110° with the trans group. Angles to both the entering ligand and the leaving ligand change linearly along the IRC over the region in which one is exchanged for the other. The same is true of the Pt−Cl and Pt−E bond distances (Figure 5a). Furthermore, the bond length difference coordinate, ΔR, for which the data points and a linear regression are shown in Figure 5a, is exceptionally linear over the entire range studied, supporting our choice of this coordinate in optimizing transition states above. The cis (or axial) ligand bond lengths Pt−X and Pt−Y, by contrast, change very little over the course of the reaction (Figure 5b). That the two otherwise identical cis ligands do not show similar changes in bond length in the cases examined here indicates, further, that the small changes observed are probably the result of asymmetric steric interactions with the nucleophile.

The behavior of the trans ligand (Figure 5b) is perhaps most interesting of all, though its movement is again quite small. Variations in the trans ligand bond length appear to be the product of two effects. The first is steric interaction with the entering and leaving ligands and reaches a maximum near the point of greatest symmetry (that is, where the T−Pt−E angle is equal to the T−Pt−Cl angle). For reaction 10, which exhibits an early transition state, this occurs somewhat after the transition state is achieved. The second effect arises from the ability of the trans ligand to stabilize the transition state by a reduction in the Pt−T bond length. This effect becomes strongest very near the transition state, where the energy of the system reaches a maximum and stabilization despite the steric consequences begins to become favorable. The net result of the two effects is a broad peak in Pt−T bond length, with its maximum near the point of greatest symmetry and a "notch" near the location of the transition state.

In summary, the timing of the transition state has been found to be determined by the relative strengths of the entering and leaving ligands, the transition state more closely resembling the complex (reactant or product) containing the weaker bonding ligand. The absence of an intermediate in two of the reactions studied has been demonstrated and the IRC shown to closely resemble the bond length difference coordinate ΔR. The cis ligands are found to play a very static role in the reactions studied, while the trans ligand plays a more dynamic role, briefly approaching the metal center and stabilizing the transition state despite the opposing force of steric repulsion.

Concluding Remarks

Our purpose in this investigation was to examine the intimate mechanism of S_N2 substitution at a square-planar Pt(II) complex. To this end, density functional theory has been applied to the investigation of a systematic and experimentally well-studied set of hydrolysis, ammoniolysis, and anation reactions involving such complexes. Our results do not support the existence of a reaction intermediate in any of the reactions studied; instead, in aqueous solution these reactions are found to proceed through a single transition state, as shown in Figure 1a. The geometry found for the transition states is not unlike that found in other theoretical studies.[9] The role of each ligand in determining the details of the geometry for both ground states and the transition state has been discussed.

The predicted activation and reaction free energies also show excellent agreement with experiment; observed trends in reaction kinetics as a function of the entering, cis, and trans ligands are reproduced in the calculated activation barriers. The calculated enthalpic and entropic components individually, however, differed significantly from the corresponding experimental values. This deviation (and its absence in the corresponding free energy values) was attributed to compensation between the enthalpic and entropic effects of weak interactions not considered in the present model, including Coulomb interactions with the counterion and modification of solvent−solvent hydrogen bonding.

Interestingly, it was found that the leaving group plays a dominant role, relative to that of the entering group, in

determining the activation barrier. This observation gives important insight into the intimate mechanism of the reaction, suggesting that the entering group is pulled in from the first solvation shell only after the leaving ligand begins to dissociate and that it is this dissociation which is most important in the activation process. Analysis of changes in bond energies during the reaction confirms this hypothesis and indicates that the leaving group has lost 90% of its ground-state bond energy (while the entering group has gained only 10% of its bond energy) when the transition state has been attained.

Analysis of the intrinsic reaction coordinate has, furthermore, indicated a much more dynamic role for the trans ligand than was expected. Over the bulk of the reaction path, the trans ligand was shown to be repelled by the combined steric effects of the nucleophile and leaving group. Very near the transition state, however, a transient shortening of the Pt−T bond was observed, which is believed to be connected with the stabilization of the transition state by the trans group. The cis ligands, by contrast, were shown to play a very static role, moving only very little through the course of the reaction.

It is important to place these results in context, for we have examined here substitution reactions involving only three ligand types, two of these quite similar in their interactions with the metal center and all in aqueous solution. The present study is therefore not intended to represent an exhaustive consideration of all possible modes of interaction but rather an investigation into a common subset. Further study involving different solvents, or stronger π-acceptors and π-donors as ligands, in particular, would be valuable to the development of a more general understanding of the mechanism.

Acknowledgment. This work has been supported by the Alberta Ingenuity Fund.

Supporting Information Available: Optimized geometries of the structures discussed (Cartesian coordinates, in Å). This material is available free of charge via the Internet at http://pubs.acs.org.

IC020294K